CO_2 Sorption of a Thin Silica Layer Determined by Spectroscopic Ellipsometry

Nieck E. Benes, Gerald Spijksma, and Henk Verweij
Laboratory of Inorganic Materials Science, Faculty of Chemical Technology & MESA$^+$ Research Institute, University of Twente, 7500 AE Enschede, The Netherlands

Herbert Wormeester and Bene Poelsema
Solid State Physics Group, Faculty of Applied Physics & MESA$^+$ Research Institute, University of Twente, 7500 AE Enschede, The Netherlands

Optical properties of a thin amorphous silica membrane and the supported γ-alumina layer on which it was coated were obtained from spectroscopic ellipsometry. The thicknesses of γ-alumina and silica layers from ellipsometric spectra were 1.654 μm and 73 nm, respectively. The porosity of the γ-alumina layer was 51%. The porosity of the silica layer (15–25%), appeared to be smaller than that of unsupported silica material prepared by a similar method. Determination of the porosity of the silica layer, however, was quite inaccurate, because optical properties of the pure material were not exactly known. Ellipsometry was also used to determine the sorption behavior of CO_2 in the γ-alumina and silica layers. For both layers the observed sorption behavior could be described by a Langmuir isotherm ($c_{CO_2,max} = 0.84$ and $2.8-3.0$ mmol$\cdot g^{-1}$, respectively), with Arrhenius-type temperature dependence (sorption heat 24.6 ± 1.0 and 27.0 ± 1.3 kJ$\cdot$ mol^{-1}, respectively). The adsorption behavior of supported and unsupported γ-alumina appeared to be similar. The heat of sorption was larger for supported thin silica layers than for unsupported bulk silica, suggesting smaller pores in the thin layer.

Introduction

State-of-the-art microporous silica membranes show high fluxes for small molecules like H_2, and high selectivities for such molecules with respect to larger ones (De Vos and Verweij, 1998a). Furthermore, inorganic silica membranes can be utilized at high temperatures in chemically aggressive environments, where organic materials fail. Applications in which silica membranes can be used are, for example, natural gas purification, molecular air filtration, selective CO_2 removal, and industrial H_2 purification. A specific application is the use in high-temperature membrane reactors to remove H_2 selectively from the reaction zone to achieve conversion enhancement in thermodynamically limited reactions. Examples of such reactions can be found in steam reforming, the water–gas shift process, and dehydrogenation of hydrocarbons (Saracco et al., 1994; Zaman and Chakma, 1994).

The resistance of the silica membrane for transport of small (fast) molecules should be as small as possible, which requires a very thin layer. Such thin defect-free layers can be achieved by dip-coating the silica onto a multilayered porous supporting structure, usually consisting of a γ-alumina layer on top of an α-alumina layer (De Vos and Verweij, 1998a). The γ-layer provides a smooth surface with sufficiently small pores to enable the formation of a silica layer from sol particles, while the α-layer provides mechanical strength. Figure 1 is a SEM micrograph of such a membrane system.

Many important properties of the amorphous silica layer are strongly dependent on the conditions employed during the dip-coating process. For instance, the drying rate and pH of the dipping solution have a large influence on the porosity of the material (Frye et al., 1986; Ashley and Reed, 1986; Brinker and Sherer, 1990, chap. 13). Furthermore, information about the sorption behavior of different gases in the microporous material is imperative for a proper description of its separation performance (Benes and Verweij, 1999). Due to the small dimensions of the membrane layers, these properties are not easily measured by standard macroscopic tech-

Correspondence concerning this article should be addressed to N. E. Benes.

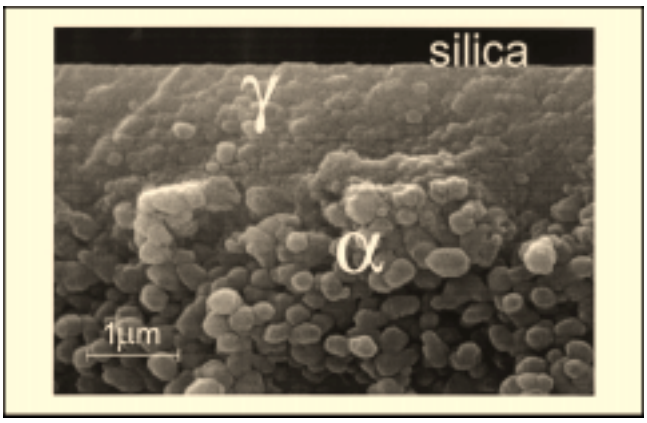

Figure 1. SEM micrograph of the cross section of a layered membrane system.

The silica layer is too thin to be visible on this scale.

niques, such as volumetric and gravimetric sorption measurements. Measuring the properties of unsupported ''bulk'' material can circumvent this problem. Although this is frequently done to investigate the effect of changes in the sol–gel process for the synthesis of the membranes (De Lange et al., 1995; Balagopal et al., 1996; De Vos et al., 1999), the properties of supported and unsupported silica are generally not identical. Microscopic techniques to obtain the structural parameters of silica include, for example, the surface acoustic wave (SAW) technique (Frye et al., 1986; Heitala et al., 1993), high-resolution solid-state NMR (Engelhardt and Michel, 1987), and ellipsometry (Tompkins, 1993). For the composite membranes studied here, the first techniques fail and only ellipsometry may be useful. Ellipsometry has been used extensively for the characterization of thin (silica) layers (Tompkins and McGahan, 1999; Cole et al., 2000). To the best of our knowledge, this technique has never been used to determine gas sorption behavior in microporous membranes.

Theory

The material under consideration is a nonconducting dielectric. When a steady electric field acts upon such a material, a small displacement of the bound charges in the atoms occurs and the atoms become polarized. A measure for this displacement is the dielectric function $\tilde{\epsilon} = \epsilon_1 + i\epsilon_2$. Light can be considered as a transverse wave consisting of both an electric- and a magnetic-field vector perpendicular to each other. In optical theory, the polarizability is expressed in terms of a refractive index $\tilde{n} = n + ik$, with $\tilde{n}^2 = \tilde{\epsilon}$, where n describes the propagation and k the absorption of light (Born and Wolf, 1986).

Reflectance

Light may be polarized in two directions: parallel to the plane of incidence, denoted *p*-polarized, and perpendicular to this plane, denoted *s*-polarized. When the light beam is reflected at a substrate, possibly with different layers on top, the polarization and intensity of the light will change. The reflectance $\tilde{r}_l(n_i, n_j)$ ($l = s$ or p) at an interface between i and j is described by the Fresnel relations (Azzam and Bashara, 1986, p. 272; Tompkins, 1993, p. 11). For a stack of thin layers the reflectance can be described in a matrix notation introduced by Abeles (Azzam and Bashara, 1986, p. 332):

$$R_l^{\text{tot}} = R_l(n_0, n_1)\, L_l(n_1, d_1)\, R_l(n_1, n_2)\, L_l(n_2, d_2)\, R_l(n_2, n_3) \ldots, \quad (1)$$

with

$$R_l(n_i, n_j) = \begin{bmatrix} 1 & \tilde{r}_l(n_i, n_j) \\ \tilde{r}_l(n_i, n_j) & 1 \end{bmatrix} \quad (2)$$

and

$$L(j) = \begin{bmatrix} e^{-[(2\pi i/\lambda)d_j]\sqrt{n_j^2 - \sin(\phi)^2}} & 0 \\ 0 & e^{-[(2\pi i/\lambda)d_j]\sqrt{n_j^2 - \sin(\phi)^2}} \end{bmatrix}, \quad (3)$$

where d_j is the thickness of layer j, λ is the wavelength of the light beam, and ϕ its angle of incidence.

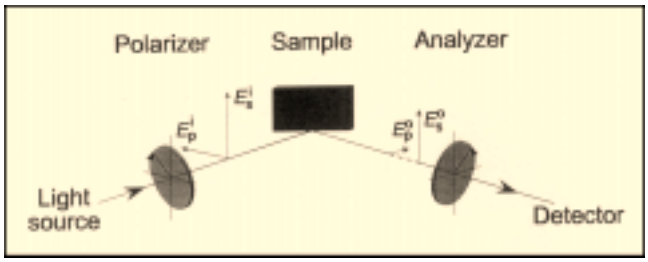

Figure 2. Top view of the spectroscopic ellipsometer.

An ellipsometer (Figure 2) measures the complex ratio $\tilde{\rho}$ of the reflectances $\tilde{r}_p^{\text{tot}}$ and $\tilde{r}_s^{\text{tot}}$. These reflectances can be derived from elements of the matrices R_p^{tot} and R_s^{tot}

$$\tilde{\rho} = \frac{\tilde{r}_p^{\text{tot}}}{\tilde{r}_s^{\text{tot}}} = \frac{R_p^{\text{tot}}[1,0]R_s^{\text{tot}}[0,0]}{R_s^{\text{tot}}[1,0]R_p^{\text{tot}}[0,0]} = \tan(\Psi)e^{i\Delta}. \quad (4)$$

This ratio is historically expressed in the real angles Ψ and Δ. The angle Δ is the change in phase difference between p and s polarized light, during reflectance. For a stack of dielectric material, such as alumina and silica, Δ remains close to 180° or 0°, depending on the angle of incidence. The rotating analyzer used in this study is rather insensitive at these values of Δ (De Nijs and Van Silfhout, 1988). Angle Ψ is the angle of which the tangent is the ratio of the magnitudes of the total reflection coefficients

$$\tan(\Psi) = |\tilde{\rho}|. \quad (5)$$

For the dielectra studied here, relevant data can be obtained by measuring only $\tan(\Psi)$ as a function of wavelength and using only this ellipsometric angle in a fit of an optical model of the sample.

Layer properties

The angle Ψ is connected to the refractive indices of the different layers and the thicknesses of the γ-alumina and silica layers. The refractive index of each layer will depend on the wavelength of the light used, the optical properties of material the layers consist of, and their porosity. The amount of gas sorbed by the material will also influence the refractive index.

Dispersion

The polarizability of atoms depends on the wavelength used. Electrons will oscillate around their equilibrium position with the frequency of the incident (driving) electric field. The strength of the oscillations is determined by the frequency difference between the driving field and an optical resonance frequency. If a resonance is within or near the wavelength range of interest, a Lorentz oscillator has to be used to characterize the dielectric response (Bijlsema et al., 1998). Because the resonance is further away, the Lorentz oscillator can be approximated by a Sellmeier form (Born and Wolf, 1986, p. 94). Still further approximation gives a Cauchy relation for the dielectric response. Substances that are transparent to the eye have no resonance wavelengths in the visible spectrum, but only in the ultraviolet or (far) infrared spectrum.

The variation of the refractive index with wavelength is referred to as dispersion. We found that the following expression sufficiently describes the dispersion of the different layers

$$n^2 = c_1 + \frac{c_2}{\lambda^2} + c_3\lambda^2. \tag{6}$$

This corresponds to a resonance wavelength in the ultraviolet range and a resonance wavelength in the infrared range. Extension of Eq. 6 with higher-order terms, or even a Sellmeier form, did not lead to better results and even showed a strong correlation between the parameters.

Effective medium approximations

The individual layers consist of a solid material with a certain refractive index, empty space (porosity), and possibly sorbed gas molecules. Although the layers are inhomogeneous on a microscopic scale, for the wavelengths considered here they may be represented by an effective medium, with an effective dielectric function $\langle\epsilon\rangle$. Many effective-medium theories have been proposed (see Kreibig and Volber, 1995, chap. 2, and references therein). The accuracy of such models is determined mainly by the degree of approximation of the topology of the sample. Extreme topologies result in the well-known Wiener boundaries for the effective dielectric function $\langle\epsilon\rangle = (1-f)\epsilon_m + f\epsilon_g$ and $\langle\epsilon\rangle^{-1} = (1-f)(\epsilon_m)^{-1} + f(\epsilon_g)^{-1}$, where m denotes the solid material, g the "gas phase" inside the material, and f the porosity. For calculating the porosity of a thin porous layer, some average of the polarizabilities of materials is made. The relation between the polarizability and the dielectric function is the so-called Lorentz-Lorenz equation, also derived for static electric fields by Clausius-Mossotti

$$\epsilon = \frac{1 + N\dfrac{2\alpha}{3\epsilon_0}}{1 - N\dfrac{\alpha}{3\epsilon_0}}, \tag{7}$$

with N the number of polarizable entities α per unit volume. For a fraction f of a phase in a host material, the Maxwell-Garnet expression (Kreibig and Vollmer, 1995, eq. 2.87) gives the effective dielectric function. This expression is, however, limited to lower values of f, where it gives approximately the same results as the formula established by Bruggeman for random mixing of two spherical components (Kreibig and Vollmer, 1995, eq. 2.89):

$$f\frac{\epsilon_g - \langle\epsilon\rangle}{\epsilon_g + 2\langle\epsilon\rangle} + (1-f)\frac{\epsilon_m - \langle\epsilon\rangle}{\epsilon_m + 2\langle\epsilon\rangle} = 0. \tag{8}$$

The balance equation derived by Bruggeman results from the self-consistent choice to represent the dielectric function of the host by that of the effective medium. This also allows for interchange of the components, which cannot be done in the framework of the Maxwell-Garnet relation. The Bruggeman expression is known to yield good results for higher values of f (Kreibig and Vollmer, 1995).

The value of ϵ_g depends on the polarizability of the sorbed CO_2 molecules. Interactions between the adsorbed molecules and the porous material may cause a change in polarizability. These interactions are relatively weak, and in this study it is assumed that the polarizabilities of sorbed and free CO_2 molecules are, to a reasonable approximation, the same. The polarizability of CO_2 per molecule, at $\lambda = 500$ nm and standard pressure and temperature, is $\alpha = 3.02\times10^{-40}\ \mathrm{F\cdot m^{-1}}$ (Bornstein, 1962, p. 6-885), with only a slight dispersion. This dispersion was used in the data evaluation. Since the number N_g of gas molecules sorbed in the respective layers will be small, the change in the effective dielectric function will be approximately linear:

$$\delta\langle\epsilon\rangle = C_1 N_g \alpha/\epsilon_0. \tag{9}$$

This linearization holds in the sorption regime studied here. For the first Wienerbound the parameter of proportionality C_1 is 1, while for the second Wienerbound $C_1 = \langle\epsilon\rangle^{-2}$. For the Bruggeman expression,

$$C_1 = \frac{1}{f}\frac{(3f-1)\langle\epsilon\rangle_0 + \epsilon_m}{2\langle\epsilon\rangle_0 + \epsilon_m/\langle\epsilon\rangle_0}, \tag{10}$$

where $\langle\epsilon\rangle_0$ is the effective dielectric function of the layer under vacuum.

Experimental Studies

The preparation of the support, γ-alumina, and silica layers is described elsewhere (Benes et al., 2000). The membranes were placed in a test cell consisting of a glass chamber surrounded by a cooling jacket, with a gas inlet and quartz

windows for the in- and outgoing light beam. Degassing of the sample was done under vacuum, and the required heat was supplied by a 50-W halogen lamp inside the cell. A reducing valve was used to control the CO_2 pressure inside the chamber.

The spectrometric ellipsometer was a rotating polarizer type equipped with a Xe lamp and photomultiplier (Wentink, 1996). A schematic representation of the ellipsometer is depicted in Figure 2. With a monochromator 101 equally spaced points in the photon energy range between 1.5 and 4 eV (λ = 830 and 310 nm, respectively) were measured. A zone angle of the analyzer of 20° was used and practically no difference between the two zones was measured. The angle of incidence was 67° and the instrument was calibrated with the so-called phase-calibration method (De Nijs and Van Silfhout, 1988).

In the fit procedure the differences between the measured tan(Ψ) and the model tan(Ψ) were minimized using the Levenberg-Marquardt nonlinear least-squares method (Press et al., 1992, p. 678). First the material properties of the α- plus γ-layer (α-γ system) were determined. After applying the silica layer, the properties of this layer were determined from the difference in spectra with the α-γ system. The properties of the α-γ system were kept constant in this fit. The CO_2 sorption experiments were also analyzed by optimizing the model to the difference in spectra with and without this gas. In the latter fits only the amount of CO_2 in the γ-alumina and silica layer were parameters.

Results and Discussion

Optical properties

The energy-dependent behavior of tan(Ψ) appeared to be independent of temperature for all samples under vacuum, from -10°C up to several hundred degrees (measured spectra and MathCad files comprising the model can be found on the World Wide Web at: http://ims.ct.utwente.nl). In Figure 3 the results are plotted for the α- plus γ-layer. The thick solid line represents the α- with no γ-layer on top. The presence of the thin γ-layer results in oscillatory behavior of tan(Ψ), due to interference effects. The thickness of this layer was found to be 1.654 μm with a numerical inaccuracy of 2 nm. This value corresponds well with the SEM micrograph of this layer. The numerical inaccuracy is obtained from the variance–covariance matrix.

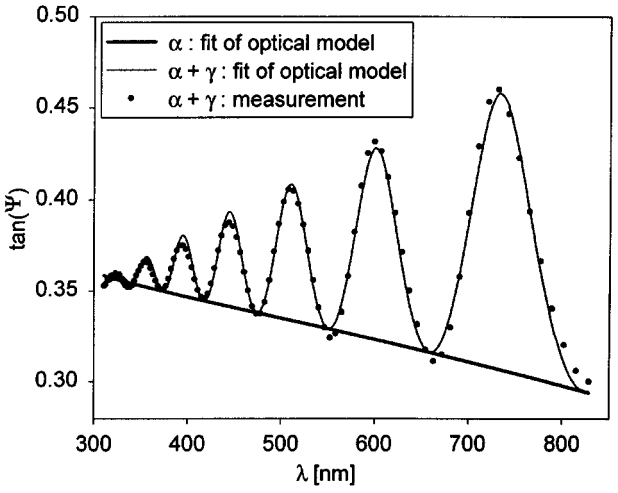

Figure 3. Wavelength dependence of tan(Ψ) for the γ-alumina layer on top of the α-alumina layer.

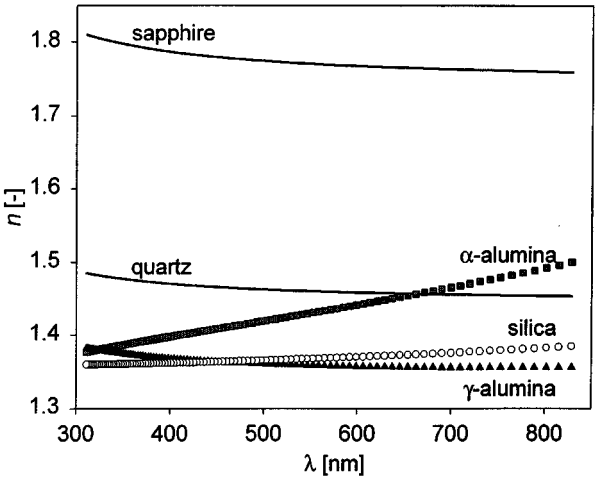

Figure 4. Dispersion of the different layers of the membrane system, pure sapphire and pure quartz.

The dispersion of the different layers, depicted in Figure 4, could be described satisfactorily using Eq. 6, with the optimized constants given in Table 1.

The support is macroporous (pore diameter $\sim$ 85 nm), and therefore simple effective medium approaches fail, as shape and pore size (distribution) influence the results. The pore diameter of the γ-layer is sufficiently small ($\sim$ 2.5 nm) and its porosity was 51% according to the Bruggeman equation. De Lange et al. (1995a) measured a slightly higher porosity ($\sim$ 55–60%) of unsupported γ-alumina material by N_2 adsorption/desorption measurements.

The measured thickness of the silica layer was 73 ± 1 nm. The inaccuracy is again obtained from the variance–covariance matrix. The thickness is in excellent agreement with FE-SEM micrographs of the layer and values obtained by De Lange et al. (1995a) for similarly prepared silica layers from SAM and XPS argon sputter profiles (60–100 nm). TEM micrographs of De Vos and Verweij (1998a), who coated the silica on top of two γ-layers, revealed a lower value of approximately 30 nm.

Compared to the γ-layer, the determination of the porosity of the silica layer using ellipsometry is not as simple a task. This is already evident from the refractive-index dispersion of the silica layer. At the lower energy side, the dispersion increases in contrast to the expected decrease. The calculation of the fraction from the Bruggeman equation using the quartz dielectric function to represent the solid material fraction results in an energy-dependent, and thus nonrealistic, porosity that ranges from 15 to 25%. Due to the —OH groups present in the silica material, the use of the quartz dielectric function is questionable and a very crude approximation at best.

Values obtained for the porosity of unsupported silica by De Lange et al. (1995a) from nitrogen physical adsorption

Table 1. Dispersion of Different Layers*

	α-Alumina	γ-Alumina	Silica
c_1	1.914	1.803	1.805
c_2	−0.00416	0.00660	0.00141
c_3	0.7721	0.0475	0.3149

*Coefficients in Eq. 6, obtained from best fits of the optical model to the measured data.

measurements are in the 35–40% range. The porosity of the supported silica film seems to be lower than that of unsupported silica material, which is in agreement with the observations of Brinker and Sherer (1990, chap. 13). They attribute denser structure of the thin silica film to the brief time span of film formation, during which only a little aging can occur.

CO_2 sorption

Figure 5 depicts the effect of sorption of CO_2 on $\tan(\Psi)$ at 0°C. Due to the sorption the oscillations are shifted slightly to the left, while the absolute value of $\tan(\Psi)$ decreases, especially for shorter wavelengths. The CO_2 sorption was determined from differences between the spectra. The change in $\tan(\Psi)$ upon sorption of CO_2 appeared to be reversible, that is, no hysteresis was observed during a sorption/desorption cycle.

In Figure 6 the sorption of CO_2, calculated using the Bruggeman equation (Eq. 9) is depicted. The dotted lines denote Langmuir isotherms fitted to the data. The maximum adsorption capacity for the γ-layer was $c_{CO_2,max} = 0.84$ mmol/g. Determining the maximum sorption capacity of the silica layer is less straightforward, because the optical properties of the solid material, and consequently the void fraction, are difficult to establish. Fortunately, the maximum sorption capacity depends only slightly on the void fraction. However, the value of the refractive index of the material is important. Assuming that the optical properties of the solid material are identical to those of quartz, and a void fraction of 20–25%, a maximum sorption of $c_{CO_2,max} = 2.8$ to 3.0 mmol/g was found. This value is probably too high. An alternative value can be obtained from the logarithmic mixing rule used in effective medium approximation theory: $\ln\langle\epsilon\rangle = \Sigma_l f_l \ln(\epsilon_l)$. For small deviations in the effective dielectric function as the result of CO_2 sorption, the exact value of the dielectric function of the solid material ϵ_m is not required. The parameter C_1 (Eq. 9) becomes $\langle\epsilon\rangle^{-1}$ and gives a maximum sorption of $c_{CO_2,max} = 2.29$–2.42 mmol/g. The maximum sorption capacity is in fair agreement with the values of ~ 2.7 mmol/g found by De Lange et al. (1995b) for unsupported silica, using a gravimetric high-pressure sorption setup. The shape of the curves is also very similar to that obtained by De Lange et al., using a low-pressure volumetric setup.

In Figure 7 Arrhenius plots of the CO_2 sorption are presented. In these plots the relative occupancy $\theta = c_{CO_2}/c_{CO_2,max}$ is used. Because of an approximately linear relation between the change in the dielectric function and c_{CO_2}, the normalization with respect to a maximum concentration en-

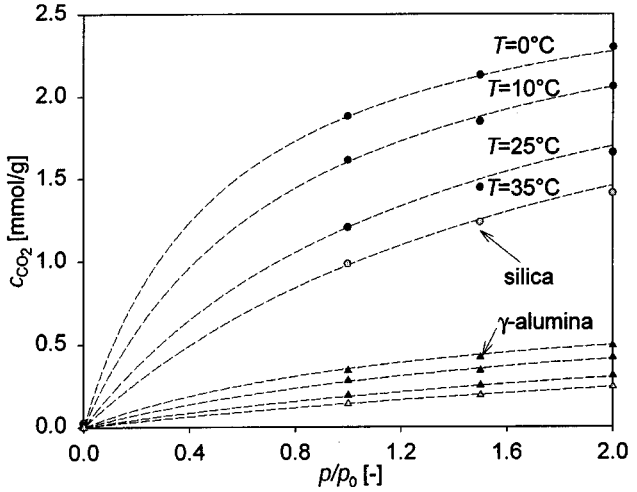

Figure 6. CO_2 isotherms, $p_0 = 1$ bar.

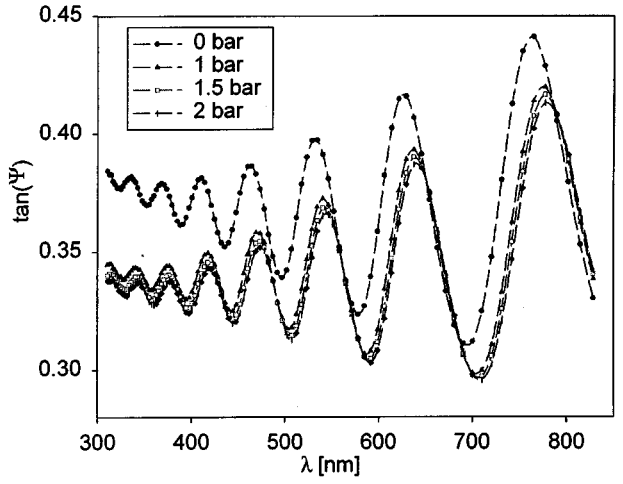

Figure 5. Effect of CO_2 sorption, in the three-layered membrane system, on $\tan(\Psi)$.

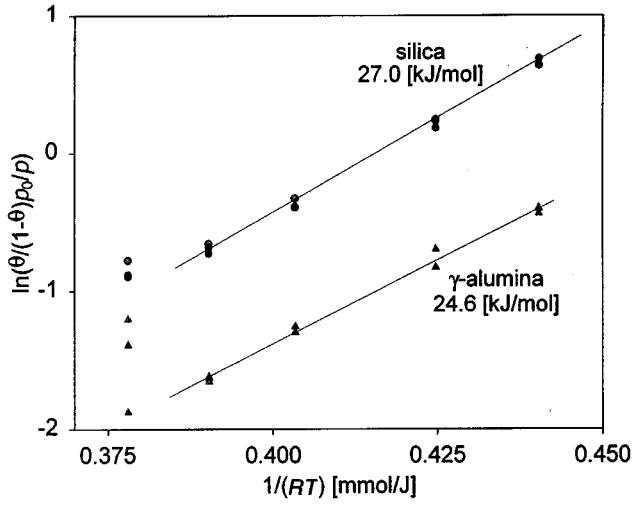

Figure 7. Arrhenius representation of CO_2 sorption in the γ-alumina and silica layers.

ables calculation of the heat of sorption without selecting an effective medium approach. The linear behavior of $\ln(\theta/(1-\theta)p_0/p)$, where $p_0 = 1$ bar, with $1/RT$, is observed, and the corresponding heats of sorption are 27.0 ± 1.3 and 24.6 ± 1.0 kJ·mol^{-1} for the silica and γ-alumina layer, respectively.

Comparison with Open Literature. The sorption of CO_2 in metal oxides has been the subject of many studies. Auroux and Gervasini (1990) studied the energetics of the adsorption of CO_2 on several simple metal oxides, including commercial γ-alumina. The latter material exhibited a remarkable chemical heterogeneity, showing an average heat of adsorption of 60 kJ·mol^{-1} for CO_2. Using the differential heat of adsorption, Auroux and Gervasini studied the basic energy distribution sites and found that a large fraction of CO_2 was physisorbed on the surface (differential heat of adsorption 25 kJ·mol^{-1}). The average value of the heat of sorption, found by Auroux and Gervasini, is relatively large compared with other data found in the literature. Uhlhorn (1990, p. 73) studied the adsorption of CO_2 on unsupported γ-alumina material, prepared in an identical way as the material studied in this work. He found that the adsorption was reversible, that is, without hysteresis, and that the isosteric heat of adsorption was relatively constant, with an average value of 26 kJ·mol^{-1}. Only after modification of the alumina with more basic metal oxides, such as MgO, did he find a large value for the heat of adsorption, combined with a hysteresis in the adsorption/desorption curve. The average value of Q_{st} found by Uhlhorn for unmodified γ-alumina bulk material is in excellent agreement with the value found here, which indicates that the adsorption of CO_2 in the unsupported and supported γ-alumina materials is similar.

The value of the heat of sorption of CO_2 in silica is also indicative of physisorption. In contrast to γ-alumina, silica is not amphoteric but rather acidic. In general, no CO_2 sorption is observed for acidic metal oxides (Auroux and Gervasini, 1990). This is apparently not the case for the silica material studied here. Physisorption studies of the morphology of microporous silica using CO_2 at -78°C give, within 10%, the same results as using N_2 at -196°C (Iler, 1979, p. 472). The sorption of N_2 is believed to be influenced by interactions of its quadrupole with the polar surface and decreases for lower silanol numbers. For CO_2 it is also observed that removal of hydroxyl groups has a negative influence on sorption (De Vos et al., 1999). The value of $c_{CO_2,max}$ found in this study is in fair agreement with that found by De Vos and Verwij (1998b) and De Lange et al. (1995b), who both studied the CO_2 sorption of unsupported silica material prepared in a manner identical to the material studied here. The similar value of $c_{CO_2,max}$ suggests that the silanol numbers of the supported and unsupported silica are similar. This is in agreement with the fact that in the synthesis of the supported and unsupported materials, only the consolidation step is different, that is, the starting materials, synthesis route, and heat treatment are identical.

Both De Lange et al. and De Vos and Verwij found a heat of sorption of 24 kJ·mol^{-1}. The higher value of the heat of sorption in the case of the thin silica layer is not likely to be due to a difference in surface chemistry (silanol number) of this layer and unsupported silica, but is in all probability associated with differences in the pore morphologies of both materials. In microporous materials overlap of the neighboring potential fields of opposing pore walls can lead to enhanced sorption, depending on the ratio of the size of the pore to that of a sorbed molecule. The pore size in unsupported silica is relatively large compared to the size of a CO_2 molecule. Consequently, the increased heat of sorption can be attributed to smaller pores in the thin silica membranes compared to those in the bulk silica. A smaller pore size in the thin layer is consistent with the fact that defect-free silica membranes show almost no permeance for methane (kinetic diameter 3.8 Å). This indicates that the pore size of these membranes is smaller than methane, while the pores in unsupported material are in the range 4–5 Å. Bhandarkar et al. (1992) studied the sorption of CO_2 in an unsupported silica material with an even larger pore size (in the 5–20 Å range) and found a heat of sorption of 18 kJ·mol^{-1}.

Limitations of the setup

Due to experimental limitations it was not possible to measure sorption behavior over a wider range of temperatures and pressures. However, this is not due to a principal limitation of the spectrometric ellipsometry technique. A cell that can withstand wider ranges of pressures and temperatures, combined with a more accurate control of these variables, should make ellipsometry a useful technique for obtaining essential sorption data of gases in thin supported layers.

Conclusions

The porosities and thicknesses of thin membrane layers deposited on a support have been measured using ellipsometry. The thickness and porosity of the mesoporous γ-alumina layer are 1.654 ± 0.002 μm and 51%, respectively, while for the microporous amorphous silica layer the obtained values are 73 ± 1 nm and 15–25%.

The sorption behavior of CO_2 has been measured at different pressures and temperatures. For both layers the sorption behavior can be described well by a Langmuir isotherm, with maximum sorption concentrations of 0.84 and 2.8–3.0 mmol·g^{-1} for the γ-alumina and silica layers, respectively. The heats of sorption are 24.6 ± 1.0 and 27.0 ± 1.3 kJ·mol^{-1} for the γ-alumina and silica layer, respectively.

Adsorption of CO_2 is similar for supported and unsupported γ-alumina. In the case of silica, the thin supported layer shows a larger heat of sorption than bulk silica. This suggests that the pores in the thin silica layer are smaller than those in the unsupported silica material.

Spectrometric ellipsometry has shown to be a useful technique for measuring sorption behavior in thin supported layers. Further improvements of the test-cell used here will enable measurements of isotherms over a wider range of pressures and temperatures.

Literature Cited

Ashley, C. S., and S. T. Reed, "Sol-Gel AR Films for Solar Applications," *Better Ceramics Through Chemistry II*, C. J. Brinker, D. E. Clark, and D. R. Ulrich, eds., Mater. Res. Soc., Pittsburgh, p. 671 (1986).

Auroux, A., and A. Gervasini, "Microcalorimetric Study of the Acidity and Basicity of Metal Oxides Surfaces," *J. Phys. Chem.*, **94**, 6371 (1990).

Azzam, R. A. M., and N. M. Bashara, *Ellipsometry and Polarised Light*, Elsevier, Amsterdam (1986).
Balagopal, N. N., K. Keizer, W. J. Elferink, M. J. Gilde, H. Verweij, and A. J. Burggraaf, ''Synthesis, Characterisation and Gas Permeation Studies on Microporous Silica and Alumina-Silica Membranes for Separation of Propane and Polypropane,'' *J. Memb. Sci.*, **116**, 161 (1996).
Benes, N. E., A. Nijmeijer, and H. Verweij, ''Microporous Silica Membranes,'' *Recent Advances in Gas Separations with Microporous Membranes*, N. Kanellopoulos, ed., Elsevier, Amsterdam (2000).
Benes, N. E., and H. Verweij, ''Comparison of Macro- and Microscopic Theories Describing Multicomponent Mass Transport in Microporous Media,'' *Langmuir*, **15**, 8292 (1999).
Bhandarkar, M., A. B. Shelekin, A. G. Dixon, and Y. H. Ma, ''Adsorption, Permeation and Diffusion of Gases in Microporous Membranes I. Adsorption of Gases on Microporous Glass Membranes,'' *J. Memb. Sci.*, **75**, 221 (1992).
Bijlsema, M. E., H. Wormeester, D. H. A. Blank, E. A. Span, A. van Silfhout, and H. Rogalla, ''Temperature Dependence of the 4eV Optical Transition in Yba2Cu3O6,'' *Phys. Rev. B*, **57**, 57 (1998).
Born, M., and E. Wolf, *Principles of Optics*, 6th ed., Pergamon Press, Oxford (1986).
Bornstein, L., *Z. Phy. Chem. Astron. Geophys. Tech.*, **6**(2), 8 (1962).
Brinker, C. J., and G. W. Sherer, *Sol-Gel Science: The Physics and Chemistry of Sol-Gel Processing*, Academic Press, Boston (1990).
Cole, D. A., J. R. Shallenberger, S. W. Novak, R. L. Moore, M. J. Edgell, S. P. Smith, C. J. Hitzman, J. F. Kirchhoff, E. Principe, W. Nieveen, F. K. Huang, S. Biswas, R. J. Bleiler, and K. Jones, ''SiO_2 Thickness Determination by X-Ray Photoelectron Spectroscopy, Auger Electron Spectroscopy, Secondary Ion Mass Spectrometry, Rutherford Backscattering, Transmission Electron Microscopy, and Ellipsometry,'' *J. Vac. Sci. Technol. B*, **18**, 440 (2000).
De Lange, R. S. A., J. H. A. Hekkink, K. Keizer, and A. J. Burggraaf, ''Formation and Characterization of Supported Microporous Ceramic Membranes Prepared by Sol-Gel Modification Techniques,'' *J. Memb. Sci.*, **99**, 57 (1995a).
De Lange, R. S. A., J. H. A. Hekkink, K. Keizer, A. J. Burggraaf, and Y. H. Ma, ''Sorption Studies of Microporous Sol-Gel Modified Ceramic Membranes,'' *J. Porous Mat.*, **2**, 141 (1995b).
De Nijs, J. M. M., and A. van Silfhout, ''Systematic and Random Errors in Rotating-Analyzer Ellipsometry,'' *J. Opt. Soc. Amer.*, **5**, 773 (1988).
De Vos, R. M., and H. Verweij, ''High-Selectivity, High-Flux Silica Membranes for Gas Separation,'' *Science*, **279**, 1710 (1998a).
De Vos, R. M., and H. Verweij, ''Improved Performance of Silica Membranes for Gas Separation,'' *J. Memb. Sci.*, **143**, 37 (1998b).
De Vos, R. M., W. F. Maier, and H. Verweij, ''Hydrophobic Silica Membranes for Gas Separation,'' *J. Memb. Sci.*, **158**, 277 (1999).
Engelhardt, G., and D. Michel, *High Resolution Solid State NMR of Silicates and Zeolites*, Wiley, New York (1987).
Frye, G. C., A. J. Ricco, S. J. Martin, and C. J. Brinker, ''Characterisation of the Surface Area and Porosity of Sol-Gel Films using SAW Devices,'' *Better Ceramics Through Chemistry III*, C. J. Brinker, D. E. Clark, and D. R. Ulrich, eds., Mater. Res. Soc., Pittsburgh, p. 349 (1986).
Heitala, S. L., D. M. Smith, V. M. Heitala, G. C. Frye, and S. J. Martin, ''Pore Structure Characterisation of Thin Films Using a Surface Acoustic Wave/Volumetric Adsorption Technique,'' *Langmuir*, **9**, 249 (1993).
Iler, R. K., *The Chemistry of Silica*, Wiley, New York (1979).
Kreibig, U., and M. Vollmer, *Optical Properties of Metal Clusters*, Springer-Verlag, Berlin (1995).
Press, W. H., S. A. Teulkolsky, W. T. Vetterling, and B. P. Flannery, *Numerical Recipes in Fortran 77*, 2nd ed., Cambridge Univ. Press, Cambridge (1992).
Saracco, G., G. F. Versteeg, and W. P. M. van Swaaij, ''Current Hurdles to the Success of High-Temperature Membrane Reactors,'' *J. Memb. Sci.*, **95**, 105 (1994).
Tompkins, H. G., *A User's Guide to Ellipsometry*, Academic Press, San Diego (1993).
Tompkins, H. G., and W. A. McGahan, *Spectroscopic Ellipsometry and Reflectometry, A User's Guide*, Wiley, New York (1999).
Uhlhorn, R. J. R., ''Ceramic Membranes for Gas Separation. Synthesis and Transport Properties,'' PhD Thesis, Univ. Twente, Twente, The Netherlands (1990).
Wentink, D. J., ''Optical Reflection Studies of Si and Ge (001) Surfaces,'' PhD Thesis, Univ. Twente, Twente, The Netherlands (1996).
Zaman, J., and A. Chakma, ''Inorganic Membrane Reactors,'' *J. Memb. Sci.*, **92**, 1 (1994).

Manuscript received Mar. 27, 2000, and revision received Sept. 10, 2000.